Structural Engineering and Mechanics, Vol. 17, No. 3-4 (2004) 379-391
DOI: http://dx.doi.org/10.12989/sem.2004.17.3_4.379

Adaptive mesh refinement/recovery strategy for FEA

Chang-Koon Choi†

Department of Civil and Environmental Engineering, KAIST, Daejeon 305-701, Korea

Eun-Jin Lee‡

DPRI, Kyoto University, Gokasho, Uji, Kyoto 611-0011, Japan

Won-Jin Yu‡†

Samsung Engineering & Construction, Sungnam-Si, 463-721, Korea

(Received September 26, 2002, Accepted June 19, 2003)

Abstract. This paper deals with the development of *h*-version adaptive mesh refinement and recovery strategy using variable-node elements and its application to various engineering field problems with 2D quadrilateral and 3D hexahedral models. The variable-node elements which have variable mid-side nodes on edges or faces are effectively used in overcoming some problems in connecting the different layer patterns of the transition zone between the refined and coarse mesh. A modified recovery technique of gradients adequate for variable-node elements and proper selection of error norms for each engineering field problems are proposed. In the region in which the error is greater than the permissible refinement error, the mesh is locally refined by subdivision. Reversely, in some parts of the domain having the error smaller than the permissible recovery error, the mesh is locally recovered (coarsened) by combination. Hierarchical structures (e.g. quadtrees and octrees) and element-based storage structures are composed to perform this adaptive process of refinement and recovery. Some numerical examples of a 3D heat conduction analysis of the concrete with hydration heat and a 2D flow analysis of vortex shedding show effectiveness and validity of the proposed scheme.

Key words: adaptive FEA; mesh refinement/recovery; variable-node element; quadrilateral element; hexahedral element.

1. Introduction

The finite element method (FEM) is widely used for solving partial differential equations (PDE's) over complex domains. The quality and accuracy of the numerical results of FEM depend much upon the discretization of the domain and the type of elements used. A relatively finer mesh is used in the areas of higher gradients and a rather coarser mesh where the gradient distribution is

† Institute Chair Professor
‡ Post-Doctoral Research Associate
‡† Senior Researcher

relatively uniform. It is generally true that the initial mesh is not optimal for these well-graded meshes. The *h*-refinement is one of the most commonly used adaptive strategies that reduce the element sizes to create a finer mesh where the initial finite element model is not adequate for the prescribed error tolerance. The quadrilateral and hexahedral variable-node elements are best utilized in the adaptive *h*-refinement strategy by bisecting the element to be refined into four or eight subdivided elements. The variable-node elements which have variable mid-side nodes on edges or faces are effectively used in overcoming some problems in connecting the different layer patterns the transition zone between the refined and coarse meshes. The use of elements with variable-nodes eliminates the necessity of imposing constraints on irregular (hanging) nodes in order to enforce the inter-element compatibility. Choi and his colleagues have carried out remarkable works about the development and improvement of various variable-node elements (Choi and Park 1989, Choi and Lee 1996, Choi and Yu 1998, 1999, Choi *et al*. 2001).

In this study, the development of *h*-version adaptive mesh refinement and recovery strategy using variable-node elements and its application to various engineering field problems with 2D-quadrilateral and 3D-hexahedral models are presented. A modified recovery technique of gradients adequate for variable-node elements and proper selection of error norms for each engineering field problems are proposed. For an economical analysis of transient or nonlinear problems, in which the locations where the mesh refinements are needed change time to time, not only the mesh refinement but also the mesh recovery is needed. In region of high error, the mesh is locally refined by subdivision. In some parts of the domain, the estimated error is much lower than the average, the mesh may also be locally coarsened. Hierarchical structures (e.g. quadtrees and octrees) and element-based storage structures are composed to perform this refinement and recovery adaptive process. In order to examine the performance of this adaptive algorithm, a 2D vortex flow analysis and a heat conduction analysis for the concrete with hydration of heat are carried out with properly selected methods for recovery of gradients, error norm and refinement error.

2. Variable-node elements

2.1 Element formulation

The variable-node elements which have variable mid-side nodes on edges or faces are effectively used to preserve interelement compatibility in connecting the different layer patterns the transition zone between the refined and coarse meshes (Fig. 1). In this study, variable-node elements have linear shape functions of which slopes are discontinuous due to mid-side nodes. Therefore, the Gaussian quadrature needs to be modified to avoid a singular integral where discontinuity exists as shown in Fig. 2 (Gupta 1978). For the sake of simple programming, however, a 4×4 and a $4 \times 4 \times 4$ modified Gaussian quadrature may be used each for quadrilateral variable-node elements and hexahedral variable-node elements.

2.2 Recovery of gradient

The recovery of gradient is necessary for error estimation assuming recovered values of gradient to be exact values. The continuous smoothed (recovered) nodal values of gradient can be obtained through the superconvergent patch recovery (SPR) procedure (Zienkiewicz and Zhu 1992) that is

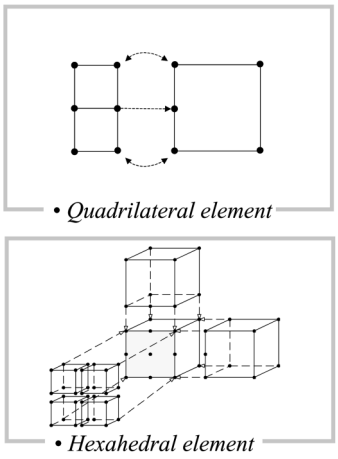

Fig. 1 Connecting the different layer patterns

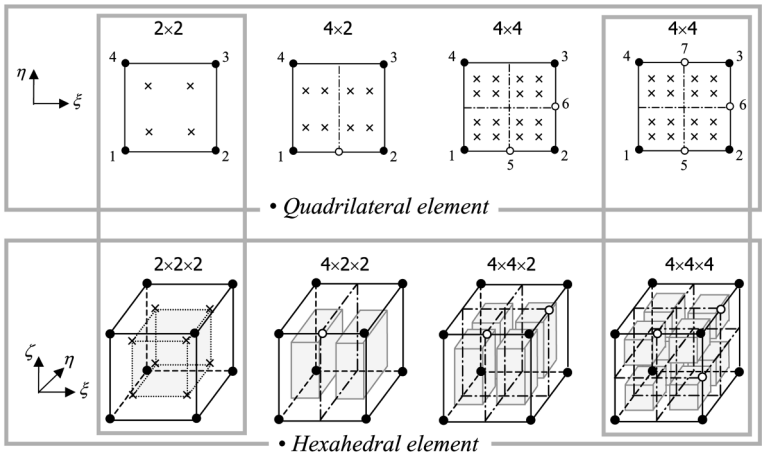

Fig. 2 Numerical integration for variable-node elements

specially modified for the variable-node elements are used in this study. Fig. 3 shows the patches composed of Gauss points of elements or sub-domains for integration surrounding the patch assembly node. For an accurate calculation of least square fit in the process of SPR, the Gauss points in the patch should be built up of a rectangular shape. In addition, the basic assumption of SPR is that these Gauss points are the optimal sampling points. But, there is no clear proof that modified Gauss points of variable-node elements are optimal even if the former results of applications using variable-node elements show good performance. So, further study is needed from the theoretical viewpoint.

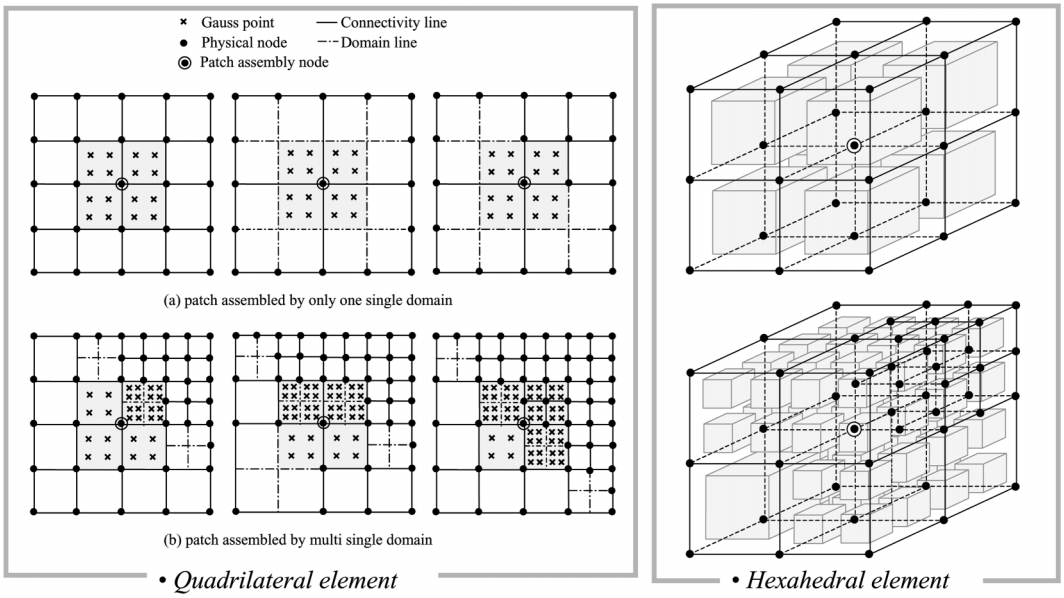

Fig. 3 Patch assembly for variable-node elements

2.3 Error estimation

Relative error estimation (Zienkiewicz and Zhu 1987) is used in this paper. The relative percentage error of the entire solution domain is estimated using the suitable error norm to the kind of each analysis.

$$\eta = \frac{\|\mathbf{e}\|}{\|\mathbf{u}\|}\times 100(\%) = \frac{\|\mathbf{e}\|}{\sqrt{\|\hat{\mathbf{u}}\|^2 + \|\mathbf{e}\|^2}}\times 100(\%) \quad \text{where} \quad \|\hat{\mathbf{u}}\|^2 = \sum_{i=1}^{nel}\|\hat{\mathbf{u}}\|_i^2, \quad \|\mathbf{e}\|^2 = \sum_{i=1}^{nel}\|\mathbf{e}\|_i^2 \tag{1}$$

The local refinement error indicator for *i*-th element η_i is defined in a similar way as

$$\eta_i = \left(\frac{\|\mathbf{e}\|_i^2}{(\|\hat{\mathbf{u}}\|^2 + \|\mathbf{e}\|^2)/nel}\right)\times 100(\%) \tag{2}$$

3. Refinement and recovery technique

3.1 h-version Adaptive FEM

Flow chart of an brief *h*-version Adaptive FEM is given in Fig. 4. In a transient or a nonlinear problem, the regions of activity vary with time and a dynamic adaptive mesh is need to capture this. In the region of higher error than the permissible refinement error e_{rf}, the mesh is locally refined by subdivision. In some parts of the domain with lower error than the permissible recovery error e_{rc}, the mesh may also be locally coarsened to recover the earlier mesh by element combination. The refinement/recovery is not performed every time step of analysis for efficiency and the frequency of refinement/recovery will depend on the nature of the problem (Choi and Yu 1999).

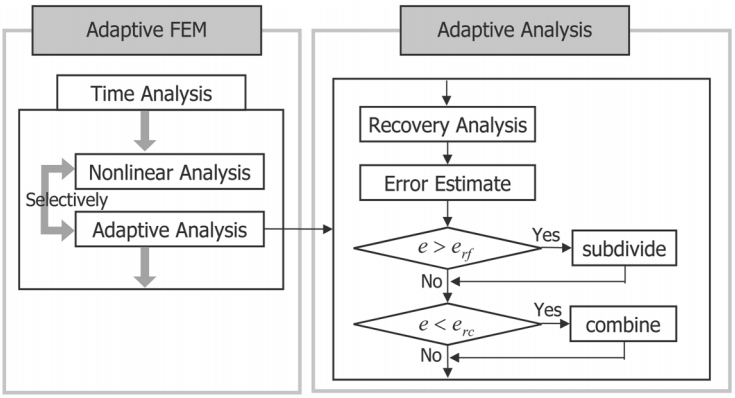

Fig. 4 Flow chart of *h*-version Adaptive FEM

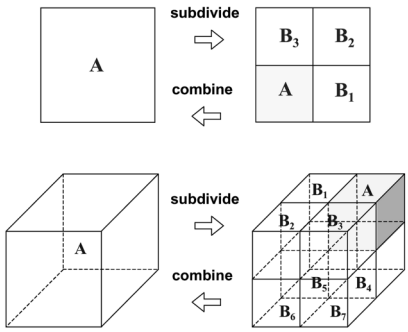

Fig. 5 Subdivide/combine

3.2 Single-level difference rule

Single-level difference rule (SLDR) is also introduced to preserve the gradual variation of sizes of element in the mesh. Indeed, SLDR (*a.k.a.* 1-irregularity) is commonly used in the *h*-version adaptive algorithm (Choi and Yu 1998, 1999). Fig. 6 shows the procedure of applying SLDR for 3D hexahedral variable-node elements. If element A has to be refined (Fig. 6(a)), its neighbor elements N_1, N_2, N_3 should be refined first (Fig. 6(b)), because of preserving the maximum difference of refinement level between neighbor elements to be 1. The same rule is applied for the recovery stage. If the divided elements of which mother element is N_1 have to be combined (Fig. 6(c)), the daughter elements of element A have to be combined first (Fig. 6(d)).

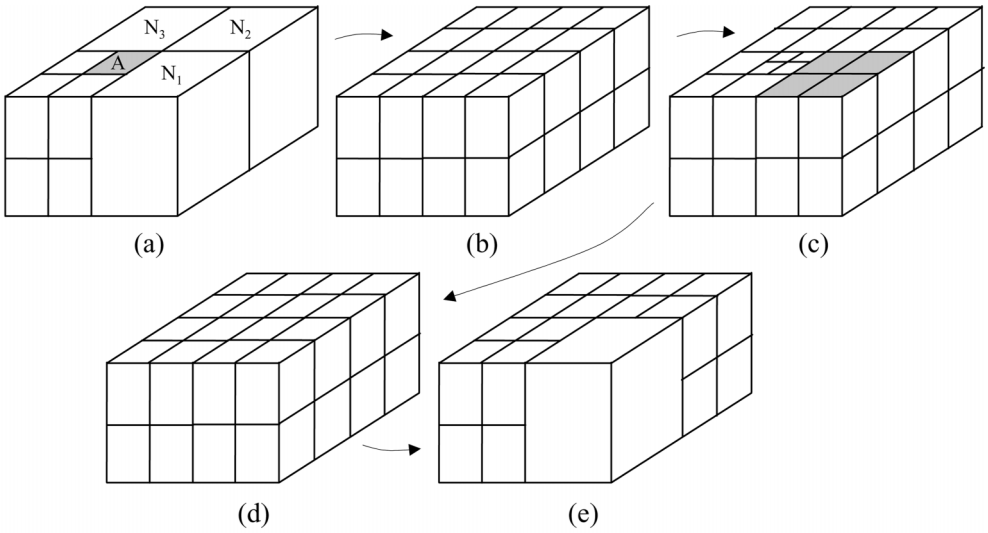

Fig. 6 Single-level difference rule

3.3 Data storage structures

In this study, an element-based data structure and direct access files are used to reduce the memory for the storage of mesh data. Fig. 7 and Fig. 8 show a simple example of the refinement history for hexahedral variable-node elements. As the 'history' of mesh refinement is not stored, the recovery of the initial mesh after refinement and coarsening is not guaranteed.

To develop an effective and systematic refinement/recovery algorithm, introduction of the tree structure of element refinement history called octuple tree (like as quadruple tree for quadrilateral elements) as shown in Fig. 8 is needed. The steps of element modifications of the same mesh are also shown in Fig. 8. For computer implementation of an octuple tree at the different time steps, M8TREE (1:ITREE), one-dimensional array, is provided as shown in Fig. 9. Now, pointers of levels, LV_ADR (1:MAXLVL) which indicate the ending location of a specified level in the M8TREE, are introduced as in Fig. 9.

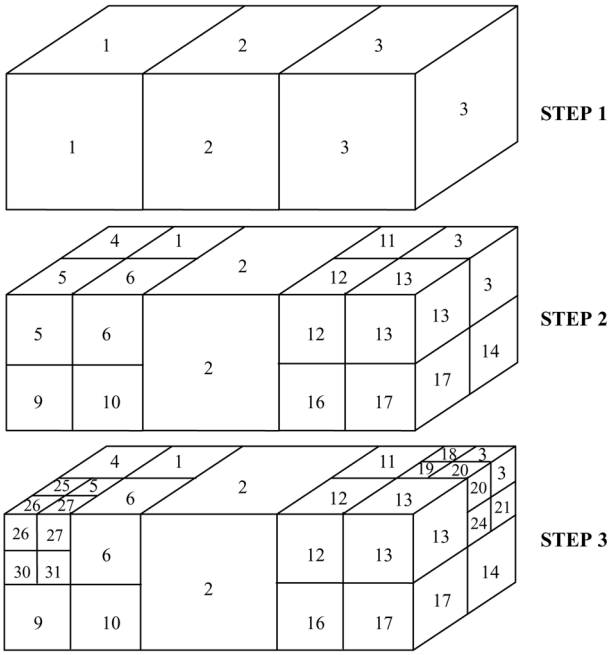

Fig. 7 Refinement history

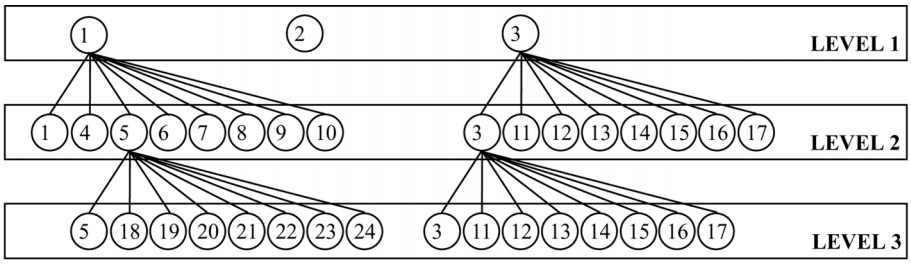

Fig. 8 Octuple tree

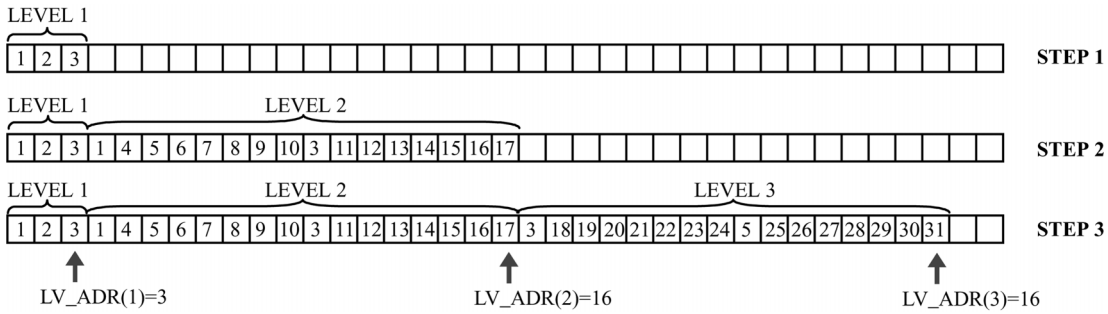

Fig. 9 M8TREE array

4. Numerical analysis

4.1 2D Flow analysis

Table 1 shows general information for adaptive 2D flow analysis (Choi and Yu 1999). In this study, penalty function formulation is used for 2D incompressible Navier-Stokes equation and basically unsteady nonliner analysis of convective term [*C*] is performed.

Table 1 General information for adaptive 2D flow analysis

Governing equation (incompressible Navier-Stokes equation)	$[M]\begin{Bmatrix}\dot{u}\\ \dot{v}\end{Bmatrix}+[[C]+[K]+\lambda[L]]\begin{Bmatrix}u\\ v\end{Bmatrix}=\begin{Bmatrix}R_u\\ R_v\end{Bmatrix}$ where λ is a penalty parameter
Variable, derivatives	$u, v, \nabla u = \partial u/\partial x, \partial u/\partial y, \nabla v = \partial v/\partial x, \partial v/\partial y$
Error norm (L_2 norm)	$\|\mathbf{e}_{\nabla u,\nabla v}\|_i = (\int_{\Omega_i}(\nabla u^* - \nabla u_h)^T\cdot(\nabla u^* - \nabla u_h)d\Omega + (\nabla v^* - \nabla v_h)^T\cdot(\nabla v^* - \nabla v_h)d\Omega)^{1/2}$
Refinement error	$\eta_i = \left(\dfrac{\|\mathbf{e}_{\nabla u,\nabla v}\|_i}{(\|\hat{\mathbf{a}}\|^2 + \|\mathbf{e}_{\nabla u,\nabla v}\|^2)/nel}\right)^{1/2}\times 100(\%)$ where $\|\hat{\mathbf{a}}\|^2 = \sum_{i=1}^{nel}(\int_{\Omega_i}(\nabla u_h^T\cdot\nabla v_h + \nabla u_h^T\cdot\nabla v_h)d\Omega)$, $\|\mathbf{e}_{\nabla u,\nabla v}\|^2 = \sum_{i=1}^{nel}\|\mathbf{e}_{\nabla u,\nabla v}\|_i^2$

The problem statement of a bluff body in a crossflow and the boundaries of problem are depicted in Fig. 10. In the problem, the singularities exist at the corners of the bluff body and may cause a separation of flow which may increase the instability of the flow and therefore decrease the accuracy of solution at those places. The various properties and control variables are given in Fig. 11. The reconstructed meshes and streamlines depicted at from t = 22.5 to 24.6 (1/2 period) are shown in Fig. 12. The main purpose of this example is to show the capability of proposed scheme to form the adaptively refined mesh near the body and in the following vortex street.

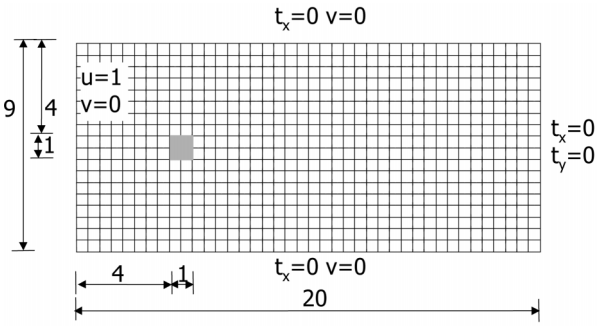

Fig. 10 Initial mesh & boundary conditions

ρ =1, μ =0.01, Re=100, Δt =0.05

artificial small disturbance at t=1

η_{rc} =25 %, η_{rf} =12.5 %

Fig. 11 Properties and control variables

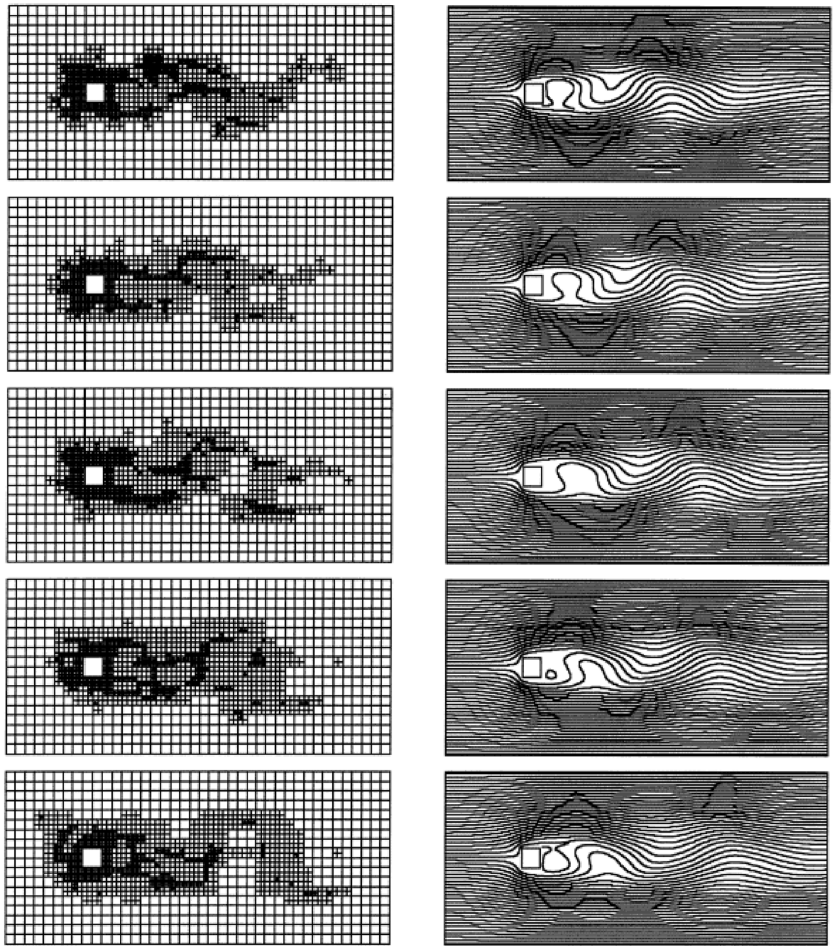

Fig. 12 Meshes and Streamlines (vortex shedding)

4.2 3D heat conduction analysis

Table 2 shows general information for 3D heat conduction analysis. In this study, unsteady linear 3D analysis is performed.

Table 2 General information for adaptive heat conduction analysis

Governing equation	$[C]\dot{T}+[K]T=\{R\}$
Variable, derivatives	$T, \nabla T = \partial T/\partial x, \partial T/\partial y, \partial T/\partial z$
Error norm (L_2 norm)	$\|\mathbf{e}_{\nabla T}\|_i = (\int_{\Omega_i} (\nabla T^* - \nabla T_h)^T \cdot (\nabla T^* - \nabla T_h) d\Omega)^{1/2}$
Refinement error	$\eta_i = \left(\dfrac{\|\mathbf{e}_{\nabla T}\|_i}{(\|\hat{\mathbf{a}}\|^2 + \|\mathbf{e}_{\nabla T}\|^2)/nel} \right)^{1/2} \times 100(\%)$ where $\|\hat{\mathbf{a}}\|^2 = \sum_{i=1}^{nel} (\int_{\Omega_i} \nabla T_h^T \cdot \nabla T_h d\Omega)$, $\|\mathbf{e}_{\nabla T}\|^2 = \sum_{i=1}^{nel} \|\mathbf{e}_{\nabla T}\|_i^2$

To show the efficiency of 3D *h*-adaptive scheme, heat conduction analysis for the concrete with heat of hydration is performed. Fig. 13 shows 3D model of the concrete monolith on the rock foundation (Ayotte *et al.* 1997). Also, thermal properties and variations of temperature on boundaries and heat of hydration are given in Table 3 and Fig. 14.

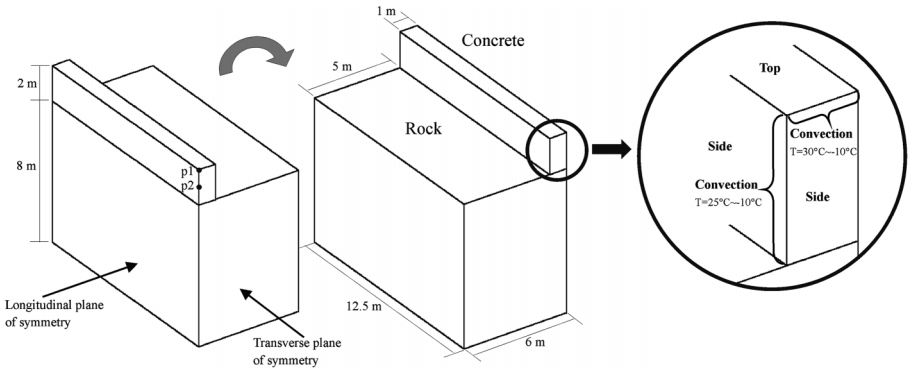

Fig. 13 3D model of concrete monolith (Ayotte *et al.* 1997)

Table 3 Thermal properties used in the analyses (Ayotte *et al.* 1997)

Thermal properties		Concrete	Rock foundation
Weight per unit volume, kg/m^3		2370	2760
Specific heat, J/kg · ^{o}C		1006	670
Thermal conductivity, W/m · ^{o}C		2.0	2.6
Convection coefficient, /m^2 · ^{o}C	· with formwork	4.8	–
	· exposed	23	–

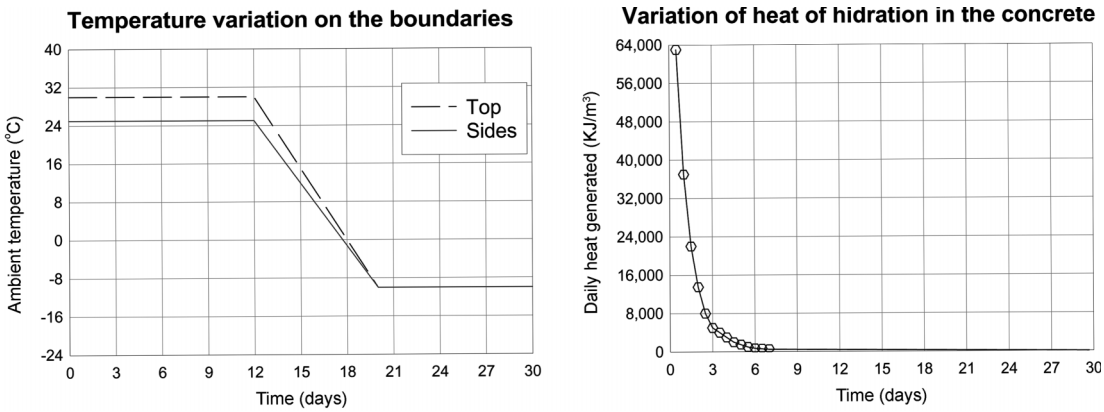

Fig. 14 LC & BC w/ time (Ayotte *et al.* 1997)

The size of the time step is 0.5 day, α is 0.5, and total analysis time is 30 days. The mesh refinements and recoveries have been performed every 0.5 days of analysis and the error criterion for refinement and recovery of an element are 40% and 4%, of which values are decided arbitrarily.

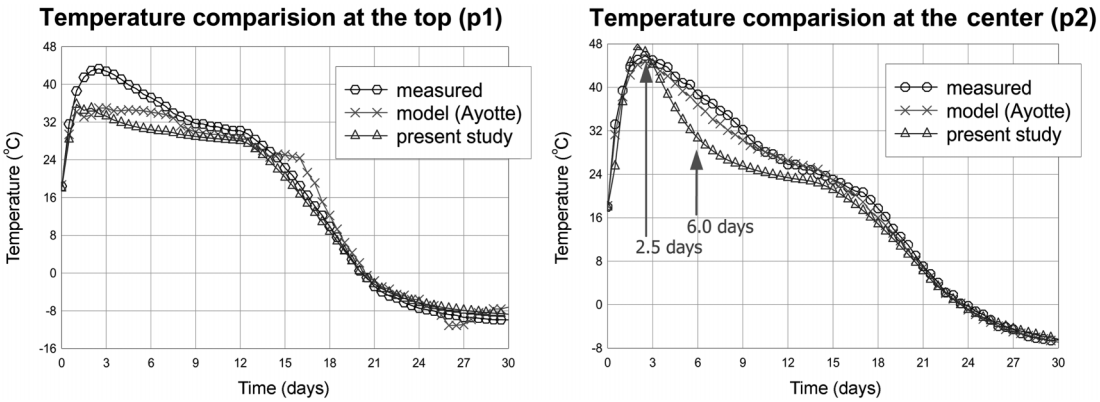

Fig. 15 Temperature variations at the top (p1) and the center (p2)

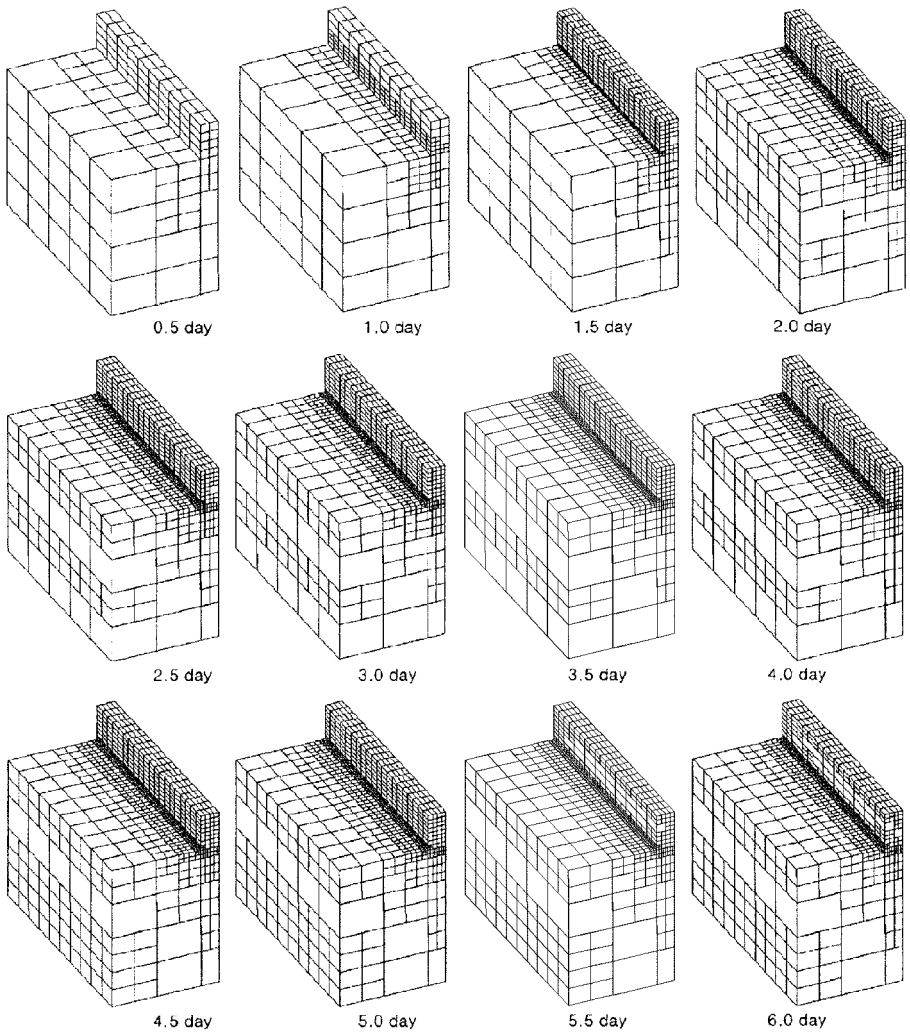

Fig. 16 Adaptive mesh forming process (0.5 day~6.0 day)

Fig. 15 shows the temperature variation at the top (p1) and the center (p2) for 30 days. The slight difference between the results of this study and other results may depend on the inconsistency of modelling conditions that is not clearly defined. The adaptive mesh generation results are shown in Fig. 16. The meshes of 5.5 day and 6.0 day are to show the recovery process. These isotherms of temperature contours (Fig. 17) show good agreements that maximum temperature generated at 2.5 day and the overall temperature distribution after 2.5 day decreased in the concrete monolith.

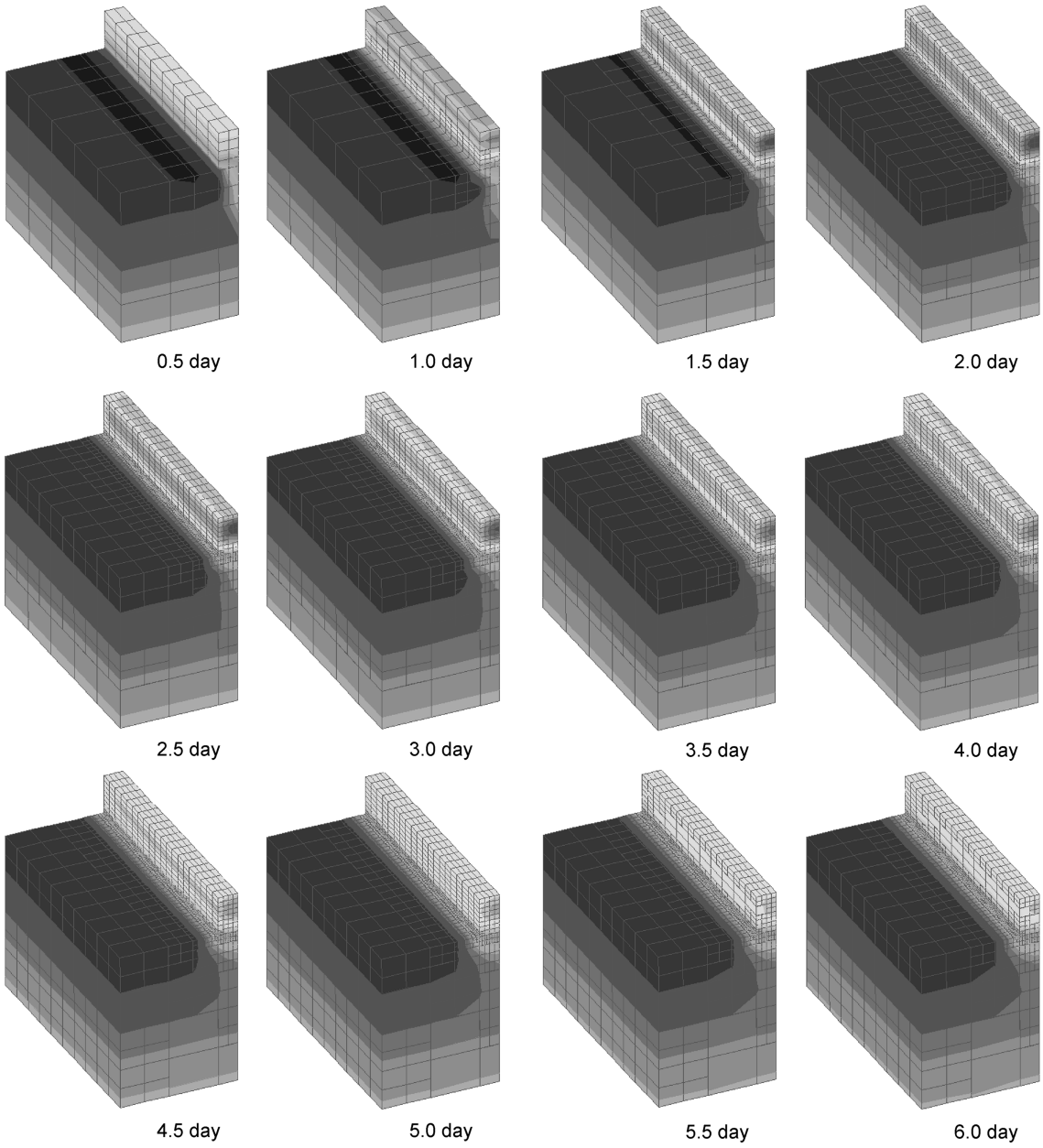

Fig. 17 Temperature contours (0.5 day~6.0 day)

The convergence curve from 0.5 day to 6.0 day, of which plot the relative percentage error of whole solution domain versus the number of equations, is given in Fig. 18(a). Because the curve after 2.0 day is not distinguishable, the linear-linear scalized convergence curve from 2.5 day to 6.0 day is given in Fig. 18(b). In this study, it is shown that the adaptive analysis has the convergence with an oscillating form through mesh refinement/recovery process.

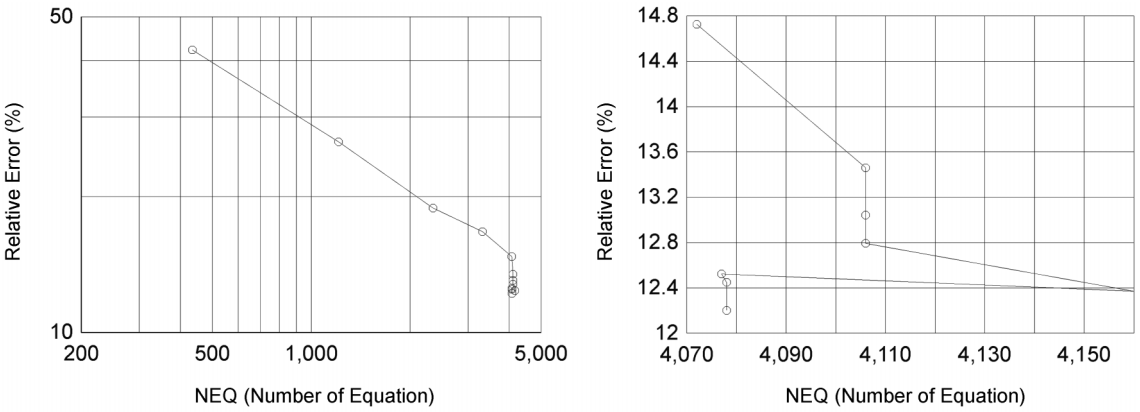

Fig. 18 Convergence Curve (0.5 day~6.0 day)

5. Conclusions

In this study, *h*-version adaptive mesh refinement and recovery strategy using variable-node elements and its application to various engineering field problems with 2D-quadrilateral and 3D-hexahedral models are presented. The variable-node element is effectively used in the *h*-adaptive mesh refinement by connecting a locally refined mesh to the existing coarse mesh through a minimum mesh modification in the transition zone. Some modification of recovery of gradient for variable-node elements used for error estimation with properly selected error norm. An effective and systematic *h*-adaptive refinement/recovery algorithm with quadruple and octuple tree data structure in one-dimensional array is presented. The validity and applicability of this *h*-refinement/recovery scheme using variable-node elements are well demonstrated through various engineering filed problems like as a 2D vortex flow analysis and a 3D heat conduction analysis for the concrete with hydration of heat.

References

Choi, C.K. and Park, Y.M. (1989), "Nonconforming transition plate bending elements with variable mid-side nodes", *Comput. Struct., An Int. J.*, **32**(2), 295-304.

Choi, C.K. and Lee, N.H. (1996), "A 3-D adaptive mesh refinement using variable-node solid transition elements", *Int. J. Numer. Meth. Eng.*, **39**(9).

Choi, C.K. and Yu, W.J. (1998), "Adaptive finite element wind analysis with mesh refinement and recovery",

Wind Struct., An Int'l J., **1**(1).
Choi, C.K. and Yu, W.J. (1999), "Finite element techniques for wind engineering", *J. Wind Eng. Ind. Aerodyn.*, **81**, 83-96.
Choi, C.K., Lee, E.J. and Lee, W.H. (2001), "Variable-node axisymmetric solid element and its application to adaptive mesh refinement", *Struct. Eng. Mech.*, **11**(4), 443-460.
Gupta, A.K. (1978), "A finite element for transition from a fine to a coarse grid", *Int. J. Numer. Meth. Eng.*, **12**, 35-45.
Ayotte, E., Massicotte, B., Houde, J. and Gocevski, V. (1997), "Modeling the thermal stresses at early ages in a concrete monolith", *ACI Mat. J.*, **94**(6), 577-587.
Zienkiewicz, O.C. and Zhu, J.Z. (1992), "The superconvergent patch recovery and a posteriori error estimates. Part 1:The recovery technique", *Int. J. Numer. Methods Eng.*, **33**, 1331-1364.
Zienkiewicz, O.C. and Zhu, J.Z. (1987), "A simple error estimator and adaptive procedure for practical engineering analysis", *Int. J. Numer. Methods Eng.*, **24**, 337-357.